Eur. J. Mech., B/Fluids, **13**, n° 2, 139-164, 1994

Resonantly interacting modes in wake-shear layers

D. WALLACE *, L. G. REDEKOPP * and P. HUERRE **

ABSTRACT. – The resonant interaction between the sinuous and varicose modes of a wake is studied for a family of velocity profiles with symmetry-breaking perturbations. The leading-order nonlinear interaction, which vanishes identically for symmetric wake profiles, increases dramatically as a small velocity ratio is imposed across the wake. Coefficients of the coupled amplitude equations describing the interaction in flows with asymmetric mean profiles are evaluated numerically for finite Reynolds numbers. The dynamical system defined by these equations is analyzed for temporally-forced, spatially-evolving modes for a velocity ratio where the flow is convectively unstable. The leading-order model is shown to be inadequate to describe the dynamical interactions for at least a limited range of velocity ratios.

1. Introduction

The dynamics of the large-scale features of spatially-developing shear flows like mixing layers, jets, and wakes exhibit distinctly different spectral characteristics. These differences are believed to derive from the underlying stability properties, particularly the propagative nature of the unstable modes, of the local, developing mean flow and the nonlinear interactions between the modes accessible to the system. For example, it is well established that the sharp frequency spectra found in two-dimensional wakes at moderate Reynolds numbers are intimately linked to the presence of a domain of sufficient extent in the near wake where the sinuous mode of the mean flow profile is absolutely unstable. On the other hand, the convectively unstable mode of mixing layers between co-flowing streams renders them highly susceptible to upstream disturbances (either ambient noise or controlled inputs) and they typically exhibit broad frequency response.

The nonlinear interaction of modes at large Reynolds numbers in a shear flow is centered at critical levels where the primary nonlinear effect is the generation of mean flow corrections. The strength of these mean flow corrections depends on the symmetry properties of the basic flow profile and the nature of the eigenmodes. For example, in symmetric wake or jet flows the inflection points occur in pairs and the streamlines passing through these points have the same mean speed. The linear neutral modes for such profiles are regular at the critical levels which are coincident with the inflection

* Department of Aerospace Engineering, University of Southern California, Los Angeles, CA 90089-1191, U.S.A.

** Laboratoire d'Hydrodynamique, École Polytechnique, 91128 Palaiseau Cedex, France.

0997-7546/94/02/$ 4.00/

points. However, when the profile symmetry is broken, the streamlines passing through the inflection points necessarily have different speeds and the linear neutral modes are no longer regular, but singular. Now, the nonlinear interaction of singular modes can be expected to be much stronger than that for regular modes. In fact, the Landau constant for the self-interaction of a regular neutral mode in the viscous critical layer regime is $O(\mathrm{Re}^{1/3})$ ([Churilov & Shukhman, 1987]; [Huerre, 1987]). The corresponding result for singular neutral modes is $O(\mathrm{Re})$ [Djordjevic & Redekopp, 1993].The symmetry of the profile also influences the nature of the bifurcation at the onset of instability. Djordjevic & Redekopp [1990] have shown that the stationary bifurcation occurring in mixing layers with a symmetric mean vorticity profile changes to a Hopf bifurcation when the symmetry of the vorticity profile is broken.

The present study focuses on the nonlinear interaction of nearly resonant modes in wake flows where the profile symmetry is broken by an imposed shear across the wake. The leading-order interaction between the sinuous and varicose modes of a symmetric wake flow vanishes identically by virtue of symmetries. Hence, the wake-shear layer provides an interesting example where the effect of broken symmetry and the consequent appearance of singular inviscid neutral modes can be examined and the implications for the nonlinear interaction of modes in this context can be explored. It also provides an example of a truly open flow system, at least for a range of the relevant parameters, where spatially chaotic dynamics can be modelled and studied. A reduced model for spatial chaos in the convectively unstable domain of parameter space for a family of profiles is derived.

In a convectively unstable or open shear flow, the developing, unsteady vorticity field is created by the spatial amplification of input disturbances at the origin of the flow. As a result, open flows are expected to be extremely sensitive to external forcing. Under natural conditions with background noise acting as the forcing of the disturbance field, it may prove difficult to establish whether a given open flow admits chaotic regimes or not since the intrinsic dynamics cannot be easily distinguished from that forced by the random excitation field. Under carefully controlled conditions and with only a few well-defined excitation frequencies applied to the flow, however, one may hope to isolate the intrinsic dynamical behaviour. This is one of the motivations behind the present study where a model-based dynamical system is developed as a guide for experiments in convectively unstable wake-shear layers.

Previous experimental investigations of chaos in open flows have, for the most part, been restricted to wakes either behind bluff bodies or behind thin airfoils. It is presently unclear whether the chaotic regimes observed in unforced cylinder wakes are purely hydrodynamically generated [Sreenivasan, 1985] or the result of hydroelastic coupling phenomena between the Karman mode of oscillation in the wake and bending modes of vibration of the body [Van Atta & Gharib, 1987]. External forcing of cylinder wakes does, however, lead to chaos as a result of frequency competition between the natural shedding frequency and the external frequency [Ollinger & Sreenivasan, 1988]. In any case, Monkewitz [1988] has shown that the near wake behind a bluff body is known to be absolutely unstable and this class of flows is, therefore, not strictly speaking "open" according to the definition adopted previously. Thin airfoil wakes, by contrast, are

convectively unstable everywhere and experiments by Aref *et al.* [1987], Van Atta *et al.* [1988], and Stuber & Gharib [1988] have indicated that excitation of the flow at several incommensurate frequencies leads to a wealth of observable flow patterns.

2. Formulation

We consider a planar incompressible flow where the coordinates are chosen so that Ox is in the direction of the undisturbed stream and Oy is in the cross-stream direction. The dependent and independent variables are scaled with respect to a length l which characterizes the cross-stream scale of the layer of mean vorticity and a reference velocity scale V_0 given by the average velocity of the streams on either side of the wake-shear layer. The nondimensional velocity profile is taken as the sum of a symmetric wake component and an antisymmetric shear layer part

$$U(y; f, r) = 1 + f \operatorname{sech}^2 y + r \tanh y. \tag{1}$$

For simplicity, the length scale l is chosen to be the same for both the even and odd parts of the profile. The form factor f and velocity ratio r appearing in (1) are defined as

$$f = \frac{V_c - V_0}{V_0}, \qquad r = \frac{V_{\infty +} - V_{\infty -}}{2\, V_0}, \tag{2}$$

where V_c is the centerline (*i. e.*, $y = 0$) velocity and $V_{\infty \pm}$ are the ambient speeds on the sides $y \to \pm \infty$, respectively. Negative values of f correspond to wake-shear layers and positive values to jet-shear layers. When $r = 0$, the profile is that of the Bickley wake or jet which admits two linear modes, the sinuous and varicose modes, which exhibit long wave instabilities. For the nominal Bickley velocity profile $U(y) = \operatorname{sech}^2 y$, the inviscid neutral states for these modes satisfy the following relations between the frequency ω, the wave number k, and the phase speed $C = \omega/k$ (*cf.* Drazin & Reid [1981]):

$$\omega_{sB} = 2\,\omega_{vB} = 4/3, \qquad k_{sB} = 2\,k_{vB} = 2, \qquad C_{sB} = C_{vB} = 2/3. \tag{3}$$

The subscripts s and v denote the sinuous and varicose modes, respectively, whose neutral eigenfunctions for the perturbed streamfunction of the inviscid problem are

$$\begin{cases} \phi_{sB}(y) = \operatorname{sech}^2 y, \\ \phi_{vB}(y) = \operatorname{sech} y \tanh y. \end{cases} \tag{4}$$

It is evident from these relations that these modes are resonant when the flow is symmetric (*i. e.*, $r = 0$). The growth rate of the varicose mode, either temporal or spatial, together with its bandwidth of instability, is smaller than that of the sinuous mode. For this reason, the varicose mode is not normally observed unless it is forced in a regime where the flow is convectively unstable. However, it may play an important role in nonlinear energy transfer processes and the examination of this effect is one goal of the present study.

Wallace & Redekopp [1991] found that the effect of a small antisymmetric component of the mean velocity profile (*i.e.*, $0<|r|<1$) caused the inviscid neutral modes to be singular. As soon as the profile symmetry is broken, the inflection points of the profile occur at different velocities and so the regularity of the function $U''(y)/(U(y)-C)$ appearing in the Rayleigh stability equation cannot be satisfied simultaneously on both sides of wake-shear layer. This is likely to have a very important effect on nonlinear interactions between the marginal modes which, at least for small values of $|r|$, are (nearly) in harmonic resonance [viz., equation (3)]. The enhanced interaction in flows with asymmetric velocity profiles is anticipated based on the asymptotic description of the dynamics in a critical layer for large Reynolds numbers. In a viscous or nonlinear-viscous critical layer, the dominant nonlinear contribution derives from a mean flow generated in the vicinity of the critical level $y=y_c$ where $U(y_c)=C$. The self-interaction of a regular neutral mode is $O(\mathrm{Re})^{1/3}$ (*cf.* Huerre [1987]) while that for a singular neutral mode is $O(\mathrm{Re})$ [Djordjevic & Redekopp, 1993]. The nonlinear interaction between the sinuous and varicose modes in the non-symmetric flow specified by (1) may experience a similar enhancement. Of course, it should be recalled that the quadratic nonlinear coupling between these modes in the weakly nonlinear theory for the purely symmetric wake or jet vanishes identically because of profile and eigenfunction symmetries as first demonstrated by Kelly [1968]. As a consequence, breaking of the profile symmetry is essential if quadratic interactions between the sinuous and varicose modes of $U(y; f, r)$ are to exist.

The governing equation for the flow is the two-dimensional vorticity equation

$$\left\{\frac{\partial}{\partial t}+\Psi_y\frac{\partial}{\partial x}-\Psi_x\frac{\partial}{\partial y}-\frac{1}{\mathrm{Re}}\nabla^2\right\}\nabla^2\Psi=-\frac{1}{\mathrm{Re}}U''' \tag{5}$$

where $\Psi(x, y, t)$ is the total streamfunction, $\mathrm{Re}=V_0 l/\nu$ is the Reynolds number, and the body-force term on the right-hand-side is introduced so that the parallel flow (1) satisfies the equations of motion. The latter term has no essential consequence in the analysis presented here because the time scale for diffusion of the mean flow is slow compared to the evolution time scale. The significance of the body force term is discussed by Huerre [1980, 1987].

A weakly nonlinear analysis is performed where the total streamfunction is divided into a mean flow part and a perturbation in the manner

$$\begin{aligned}\Psi(x, y, t)&=\int^y U(y')\,dy'+\varepsilon\psi(x, y, t)\\&=\int^y U(y')\,dy'+\varepsilon\{A(X, T)\phi_s(y)e^{i\theta_s}+B(X, T)\phi_v(y)e^{i\theta_v}+c.c.\}\\&\qquad+\varepsilon^2\psi^{(2)}(x, y, t, X, T)+\ldots\end{aligned} \tag{6}$$

The nondimensional perturbation amplitude is $\varepsilon(0<\varepsilon<<1)$ and $(X, T)=\varepsilon(x, t)$ are slow space and time scales. The phases θ_s and θ_v are defined by

$$\theta_s=k_s x-\omega_s t, \qquad \theta_v=k_v x-\omega_v t \tag{7}$$

where (k_s, ω_s) and (k_v, ω_v) correspond to neutral (*i. e.*, real) eigenvalue pairs for the sinuous and varicose modes, respectively, whose corresponding complex amplitude functions are $A(X, T)$ and $B(X, T)$. The analysis is carried out assuming that the Reynolds number is finite so the neutral eigenfunctions $\phi_s(y)$ and $\phi_v(y)$ are specified by the Orr-Sommerfeld equation

$$L[\phi] \equiv [(D^2 - k^2)^2 - ik\,\mathrm{Re}\{(U - C)(D^2 - k^2) - U''\}]\phi = 0, \tag{8}$$

subject to the boundary conditions that ϕ and ϕ' vanish as $y \to \pm\infty$. In equation (8) $D = d/dy$ and $C = \omega/k$. As demonstrated later, a range of velocity ratios and Reynolds numbers exist where the harmonic resonance conditions are closely satisfied. Assuming this is the case, portions of the right-hand-side of the inhomogeneous equation for $\psi^{(2)}$ lead to secular behaviour which can only be avoided by choosing the spatio-temporal evolution of $A(X, T)$ and $B(X, T)$ to satisfy

$$D_{\omega_s} A_T - D_{k_s} A_X = \alpha_n B^2 e^{i\theta_R(X, T)}, \tag{9a}$$

$$D_{\omega_v} B_T - D_{k_v} B_X = \beta_n A\tilde{B} e^{-i\theta_R(X, T)}. \tag{9b}$$

Here and in what follows, the superscript $\sim$ denotes the complex conjugate. The phase $\theta_R(X, T)$ measures the detuning from a precise 2 : 1 resonance between the modes and is defined by

$$\theta_R(X, T) = \left(\frac{2k_v - k_s}{\varepsilon}\right) X - \left(\frac{2\omega_v - \omega_s}{\varepsilon}\right) T. \tag{10}$$

The phase detuning varies on the slow scales when the detuning bandwidth is $0(\varepsilon)$. The coefficients in the amplitude equations (9 *a*, *b*) are obtained via orthogonality conditions yielding the integral relations

$$D_{\omega_\alpha} = \frac{i}{k_\alpha}\int_{-\infty}^{\infty} \chi_\alpha(\phi_\alpha'' - k_\alpha^2\phi_\alpha)\,dy, \qquad \alpha = s, v; \tag{11a}$$

$$D_{k_\alpha} = -\frac{i}{k_\alpha}\int_{-\infty}^{\infty} \chi_\alpha\left\{\left(U - \frac{4ik_\alpha}{\mathrm{Re}}\right)(\phi_\alpha'' - k_\alpha^2\phi_\alpha) - U''\phi_\alpha - 2k_\alpha^2(U - C_\alpha)\phi_\alpha\right\}\phi_\alpha\,dy, \qquad \alpha = s, v; \tag{11b}$$

$$\alpha_n = \frac{k_v}{k_s}\int_{-\infty}^{\infty} \chi_s\{\phi_v\phi_v''' - \phi_v'\phi_v''\}\,dy; \tag{11c}$$

and

$$\beta_n = \int_{-\infty}^{\infty} \chi_v \left\{\begin{array}{l} \phi_s'(\tilde{\phi}_v'' - k_v^2\tilde{\phi}_v) - \tilde{\phi}_v(\phi_s''' - k_s^2\phi_s') \\ + \dfrac{k_s}{k_v}[\phi_s(\tilde{\phi}_v''' - k_v^2\tilde{\phi}_v') - \tilde{\phi}_v'(\phi_s'' - k_s^2\phi_s)] \end{array}\right\} dy. \tag{11d}$$

The functions $\chi_\alpha(y)$ are the eigenfunctions of the adjoint Orr-Sommerfeld equation at the neutral eigenvalue points $(\omega_\alpha, k_\alpha, C_\alpha)$. They are specified by the equation

$$L^A[\chi_\alpha] \equiv [(D^2 - k_\alpha^2)^2 - ik_\alpha\,\mathrm{Re}\{(U - C_\alpha)(D^2 - k_\alpha^2) + 2U'D\}]\chi_\alpha = 0, \tag{12}$$

subject to the boundary conditions that the function and its first derivative vanish as $y \to \pm\infty$.

3. Numerical results

The Orr-Sommerfeld equation (8) is taken as an eigenvalue problem with the phase speed C as eigenvalue given the wave number k and the Reynolds number. A shooting technique is employed to solve this two-point boundary-value problem. The velocity is constant in the uniform flow regions external to the shear flow and analytical forms for the eigenfunction can be obtained for these regions. Integration beginning from these regions is accomplished using the asymptotic forms for $\phi(y)$ as initial inputs and integrating, using a fourth-order Runge-Kutta scheme, toward a matching point in the shear region. Iteration on the eigenvalue C is repeated until the Wronskian of the eigenfunction and its higher derivatives at the matching point is reduced to some small value approaching zero (at least 10^{-5}, say). Since the two asymptotic solutions on either side of the shear region have much different rates of exponential decay, an orthonormalization technique is used to retain the linear independence of the solutions. Eigenvalues are also computed using the Riccati method described in Drazin & Reid [1981]. Excellent agreement (at least six significant figures) between the eigenvalues calculated using the shooting technique and those obtained by use of the Riccati method verified the accuracy of the calculations.

A first check of the Orr-Sommerfeld solver is to compare the computed eigenvalues against those obtained from analytically-derived expressions. High-Reynolds number approximations to the neutral wave number k_α and associated phase speeds C_α can be inferred from Drazin & Reid [1981], pp. 233-237. For the Bickley wake profile [*cf.* $r=0$ in eq. (1)], the two-term asymptotic results are

$$k_s^{(\infty)} = 2 - \frac{24.28}{|f|\mathrm{Re}}, \qquad C_s^{(\infty)} = 1 + \frac{2}{3}f - \frac{5.425}{\mathrm{Re}}\operatorname{sgn} f; \tag{13a}$$

$$k_v^{(\infty)} = 1 - \frac{26.36}{|f|\mathrm{Re}}, \qquad C_v^{(\infty)} = 1 + \frac{2}{3}f - \frac{3.706}{\mathrm{Re}}\operatorname{sgn} f. \tag{13b}$$

A comparison of asymptotic and computed results is shown in Table I for a wake with form factor $f=-0.75$. The agreement is seen to be progressively better as the Reynolds number increases which is consistent with the asymptotic nature of $k_\alpha^{(\infty)}$ and $C_\alpha^{(\infty)}$.

TABLE I. – Comparison of computed and asymptotic results for neutral eigenvalues of the Bickley wake.

Re	k_s	$k_s^{(\infty)}$	C_s	$C_s^{(\infty)}$	k_v	$k_v^{(\infty)}$	C_v	$C_v^{(\infty)}$
300	1.8984	1.8921	0.5175	0.5181	0.8667	0.8829	0.5097	0.5124
700	1.9550	1.9538	0.5076	0.5078	0.9474	0.9498	0.5049	0.5053
1500.	1.9787	1.9784	0.5036	0.5036	0.9761	0.9766	0.5024	0.5025

A second and more stringent test of the numerical method includes computation of the eigenfunctions. One test involving the eigenfunctions is computation of the group velocities C_{g_α} defined in terms of the integral relations (11 *a*, *b*),

$$C_{g_\alpha} = -D_{k_\alpha}/D_{\omega_\alpha} \tag{14}$$

Evaluation of C_{θ_α} by this means involves computation of the eigenfunctions $\phi_\alpha(y)$ and their second derivatives as well as the adjoint functions $\chi_\alpha(y)$. The adjoint functions in the inviscid limit are singular, being given by

$$\chi_\alpha(y) = \frac{\phi_\alpha(y)}{U(y) - C_\alpha}. \tag{15}$$

For finite Reynolds numbers, and in the linear, viscous limit being considered here, the singularity is smoothed through a viscous critical layer of characteristic scale proportional to $(k_\alpha \mathrm{Re})^{-1/3}$. For high values of the Reynolds number these layers are quite thin and it is difficult to resolve the adjoint eigenfunctions numerically in these regions. For this reason, the path of integration for the Orr-Sommerfeld and adjoint equations, as well as the integral expressions in (11), are evaluated on a deformed path in the complex y-plane. The path chosen for this study is

$$y_i = -1.3 \tanh(y_r). \tag{16}$$

The functions $\phi(y)$, $\chi(y)$, and $U(y)$ are analytic in the vicinity of the real axis for finite Reynolds numbers so no difficulties are encountered. Examples of the eigenfunctions and their adjoints are shown in Figures 1 and 2. Computations of these results were

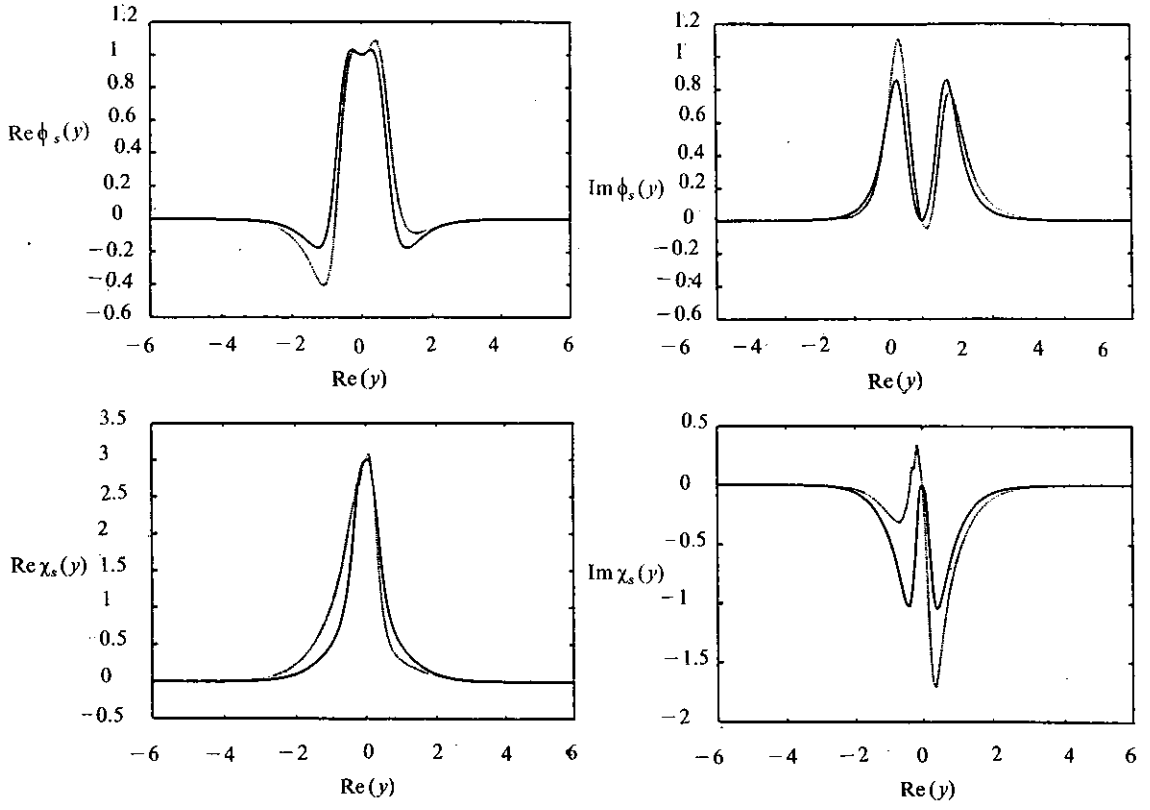

Fig. 1. – Eigenfunctions for the sinuous mode (Re = 700; $-r = 0, \ldots r = 0.12$).

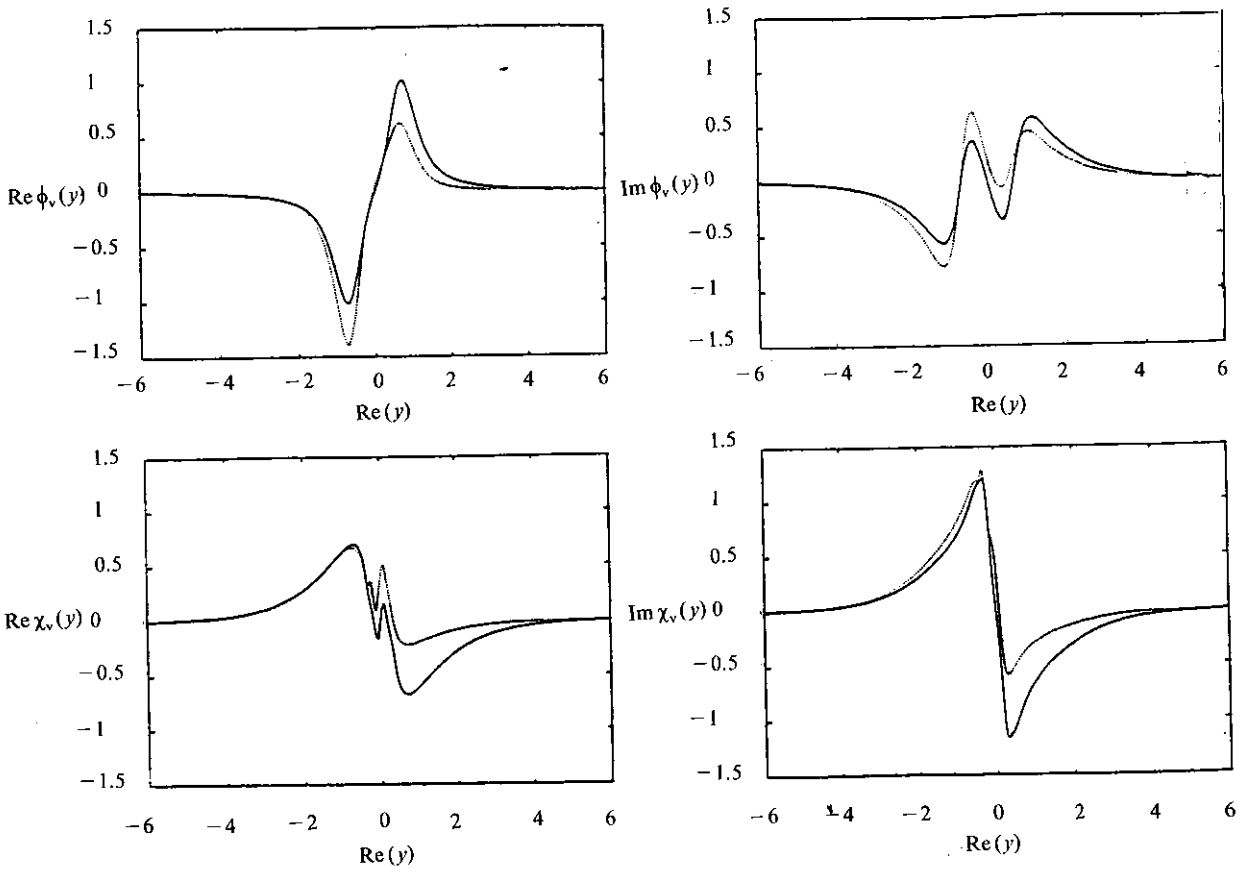

Fig. 2. — Eigenfunctions for the varicose mode (Re = 700; $-r = 0, \ldots r = 0.12$).

used to evaluate the group velocity by means of (14) using (11 *a*, *b*). The computed values were compared with the corresponding asymptotic relation which can be inferred directly from results given by Drazin & Reid [1981], pp. 233-237. The asymptotic relations are

$$C_{g_s}^{(\infty)} = 1 + 1.004\, f\left(1 - \frac{9.482}{\mathrm{Re}}\right) - 0.221\,7\, i\left(|f| - \frac{12.14}{\mathrm{Re}}\right), \tag{17a}$$

$$C_{g_v}^{(\infty)} = 1 + 0.642\,8\, f\left(1 - \frac{4.787}{\mathrm{Re}}\right) - 0.180\,6\, i\left(|f| - \frac{26.36}{\mathrm{Re}}\right), \tag{17b}$$

The data in Table II for $f = -0.75$ give reason to believe that the computed eigenfunctions are quite accurate. The largest discrepancies occur for the imaginary parts whose dominant contribution comes from the vicinity of the thin critical layer when the Reynolds number is large. In fact, the imaginary parts in the inviscid limit come from the indented contour around the critical point on the real axis. Hence, we conclude that our computed values of the coefficients defined by (11) can be accepted with reasonable confidence.

TABLE II. – Comparison of computed and asymptotic values of the group velocity for the Bickley wake.

Re	C_{gs}	$C_{gs}^{(\infty)}$	C_{gv}	$C_{gv}^{(\infty)}$
300. . .	$0.2687-0.1791\,i$	$0.2708-0.1573\,i$	$0.5451-0.1050\,i$	$0.5256-0.1196$
700. . .	$0.2567-0.1734\,i$	$0.2572-0.1624\,i$	$0.5289-0.1245\,i$	$0.5212-0.1286\,i$
1500 . .	$0.2518-0.1700\,i$	$0.2518-0.1645\,i$	$0.5229-0.1308\,i$	$0.5194-0.1323\,i$

3.1. RESONANCE CONDITIONS

Eigenvalues at finite Reynolds numbers were computed to examine how closely the exact resonance conditions (3) of the inviscid Bickley profile are approximated for profiles where the cross-stream symmetry is broken. For this purpose a generalized asymmetric velocity profile was used involving two symmetry breaking terms

$$V(y)=\operatorname{sech}^2 y+R\tanh y+P\operatorname{sech} y\tanh y. \tag{18}$$

The last term adds a shear across the wake-shear layer centerline without affecting the velocity ratio. It is included here because it has been employed to model the near-wake of a splitter plate in mixing layer experiments (*cf.* Zhang, Ho & Monkewitz [1985]) and we wish to evaluate its effect on the resonance matching conditions. The alternate velocity profile $V(y)$ is selected for eigenvalue computations since it allows for the calculation of the detuning parameters for arbitrary values of the wake-deficit parameter f. The change in reference frame between the profile $U(y)$, where

$$U(y)=1+f\,V(y), \tag{19}$$

and $V(y)$ is readily accounted for through a simple Doppler shift in the frequency. Since the wave numbers are invariant with respect to the reference frame and the scaling parameter f, the relation between the frequencies in the two frames is given by

$$\omega^{(u)}=f\,\omega^{(v)}+k. \tag{20}$$

The resonance detuning parameters for the two profiles are therefore related as follows:

$$(2k_v-k_s)^{(u)}=(2k_v-k_s)^{(v)}, \tag{21a}$$

$$(2\omega_v-\omega_s)^{(u)}=f\,(2\omega_v-\omega_s)^{(v)}+(2k_v-k_s), \tag{21b}$$

$$(C_v-C_s)^{(u)}=f\,(C_v-C_s)^{(v)}. \tag{21c}$$

Their dependence on the velocity ratio r, or the asymmetry parameter p, for arbitrary f is given by

$$r=f\,R, \qquad p=f\,P. \tag{22}$$

In this way, general resonance detuning conditions can be computed by considering the velocity profile $V(y)$.

Since our interest is focused primarily on the effect of the symmetry breaking derived from a small velocity ratio, resonance detuning results from a series of eigenvalue calculations are presented as a function of R for three different values of P in Figure 3.

The fact that the detuning is not precisely zero at $R = P = 0$ stems from the finite Reynolds number used in our viscous calculation. One observes that the detuning for $P = 0$ is relatively small for a range of velocity ratios (e.g., less than ten percent for $|R| < 0.15$). For moderate values of the wake-deficit parameter f, this covers a reasonable range of shear components across the wake. Of course, in a spatially-developing flow, the wake-deficit parameter f will decrease in the downstream direction while the velocity ratio remains fixed. It is clear that the flow will shift from a wake to a mixing layer at some downstream position. This will occur when the number of critical levels [*i.e.*, positions where $U(y_c) = C$] reduces from two to one. The boundary for this transition in the $r-f$ plane was defined by Wallace & Redekopp [1991]. One also observes from the results in Figure 3 that negative values of P (*i.e.*, P and R of opposite sign) significantly enlarge the range of velocity ratios over which the resonance is strong. When the detuning quantities in Figure 3 become large (exceeding twenty percent, say) the phase θ_R in equations (9 *a*, *b*) oscillates rapidly and the quadratic nonlinear terms will have negligible effect on the average. In this case the evolution model will necessarily have to be extended to higher-order terms (cubic nonlinearity) and one must confront the competition between the slower evolution time scale and the time scale for diffusion of the mean profile. These issues will not be pursued here.

3.2. Coefficients of the interaction equations

The preceding results show that the harmonic interaction equations (9 *a*, *b*) describe the leading nonlinear interaction of the sinuous and varicose modes for a class of wake-shear layer profiles. Consequently, it seems worthwhile to compute the coefficients in (9) to gain some insight concerning the strength of the interaction of the two modes in specific cases. Computations of the eigenfunctions and their adjoints at neutral conditions were performed using the mean flow profile (19) and the integral expressions in (11) were evaluated. Results were obtained at a Reynolds number of $Re = 700$.

The first results we present are for the coefficients α_n and β_n of the nonlinear terms as a function of the velocity ratio r at a fixed value of the wake deficit parameter $f = -0.75$ and with $p = 0$. The results are shown in Figures 4 and 5 for the sinuous and varicose mode evolution equations, respectively. We note first that these coefficients vanish identically for the Bickley profile (*i.e.*, $r = p = 0$) in the inviscid limit by symmetry considerations (*cf.* Kelly [1968]). The difference between our computed values and zero at $r = 0$ can be used as a measure of the accuracy of our eigenfunction and integral computations. It is noted that these coefficients differ significantly from zero as the profile symmetry is destroyed. This is especially true for β_n where the real and imaginery parts quickly attain large values when r departs from zero. A possible explanation lies in the fact that, as shown by Wallace & Redekopp [1991], both modes correspond to singular neutral modes for nonzero r and that the contribution from the critical level regions can be expected to be large for such cases.

Calculations of α_n and β_n were also performed for a range of the other parameters of the problem to provide some insight to the broader parametric dependence of these coefficients. The dependence on the wake-deficit parameter at fixed velocity ratio is shown in Figures 6 and 7. Results were obtained for values of f in the range $f > -0.9$

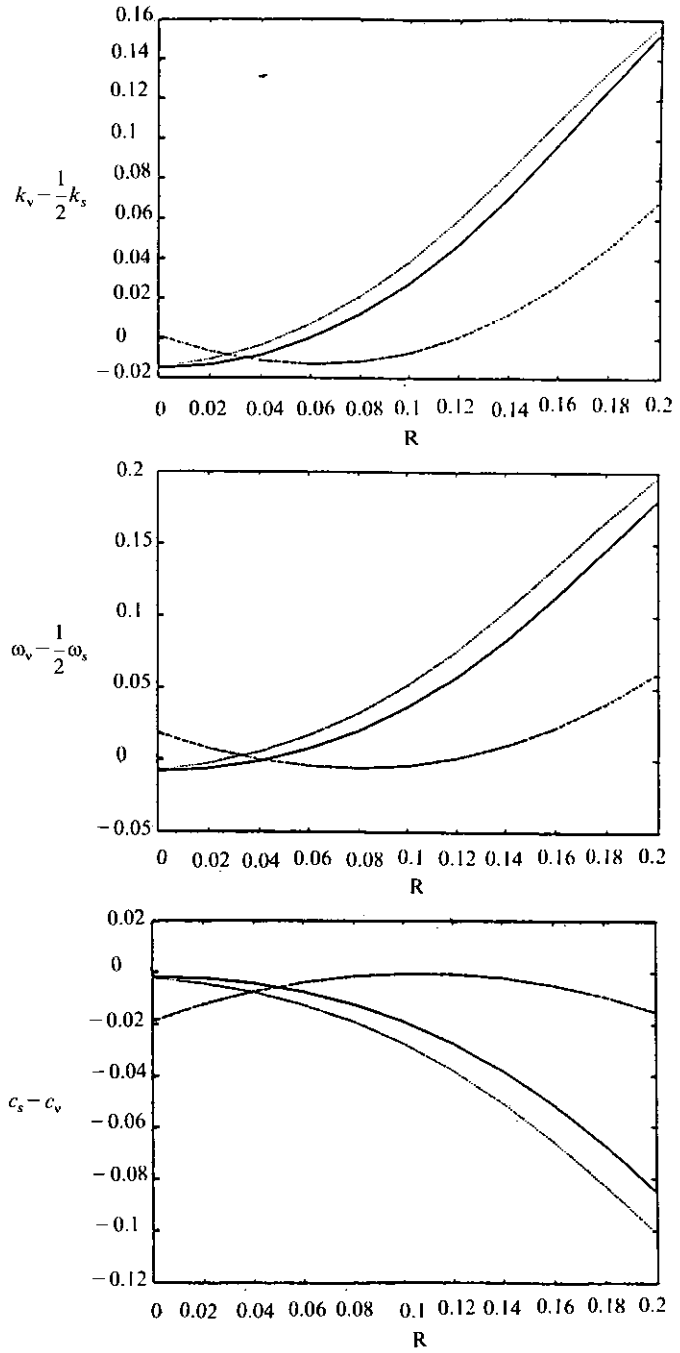

Fig. 3. — Resonance detuning conditions (Re = 1,000; −P = 0, . . . P = 0.05, --●--P = −0.25).

where the wake-shear layer is convectively unstable. The boundary between the absolute and convective instability regions in $r-f$ space was determined by Wallace & Redekopp [1991]. It is in the convectively unstable range where the model (9) for marginal modes

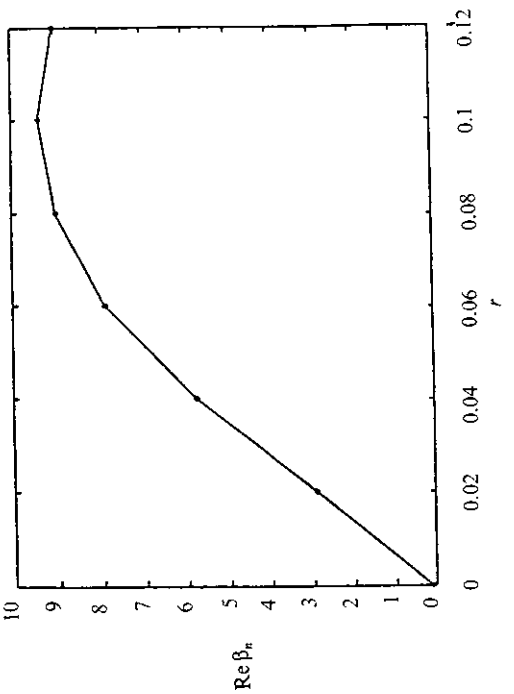

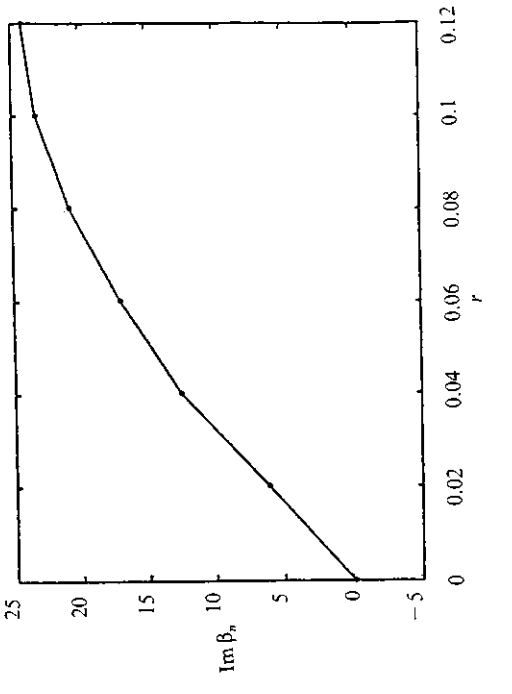

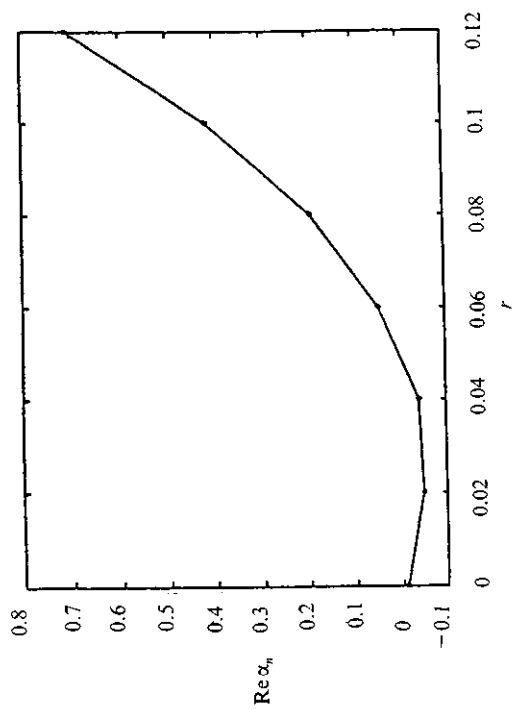

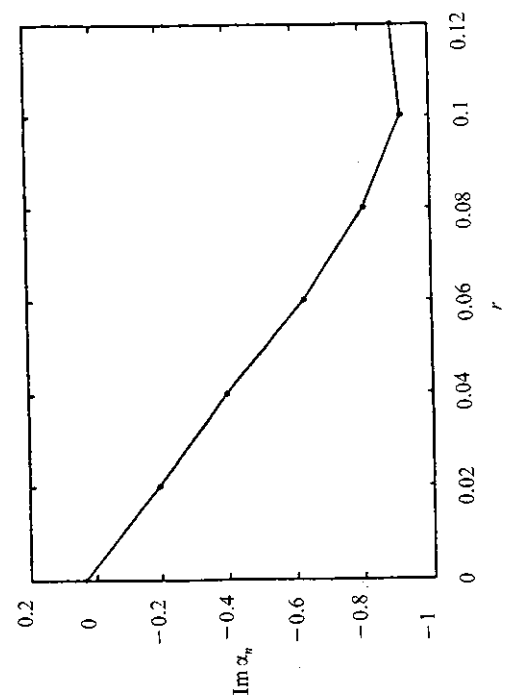

Fig. 4. – Variation of the nonlinear interaction coefficient with velocity ratio for the sinuous mode ($f = -0.75$, $p = 0$, Re = 700).

Fig. 5. – Variation of the nonlinear interaction coefficient with velocity ratio for the varicose mode ($f = -0.75$, $p = 0$, Re = 700).

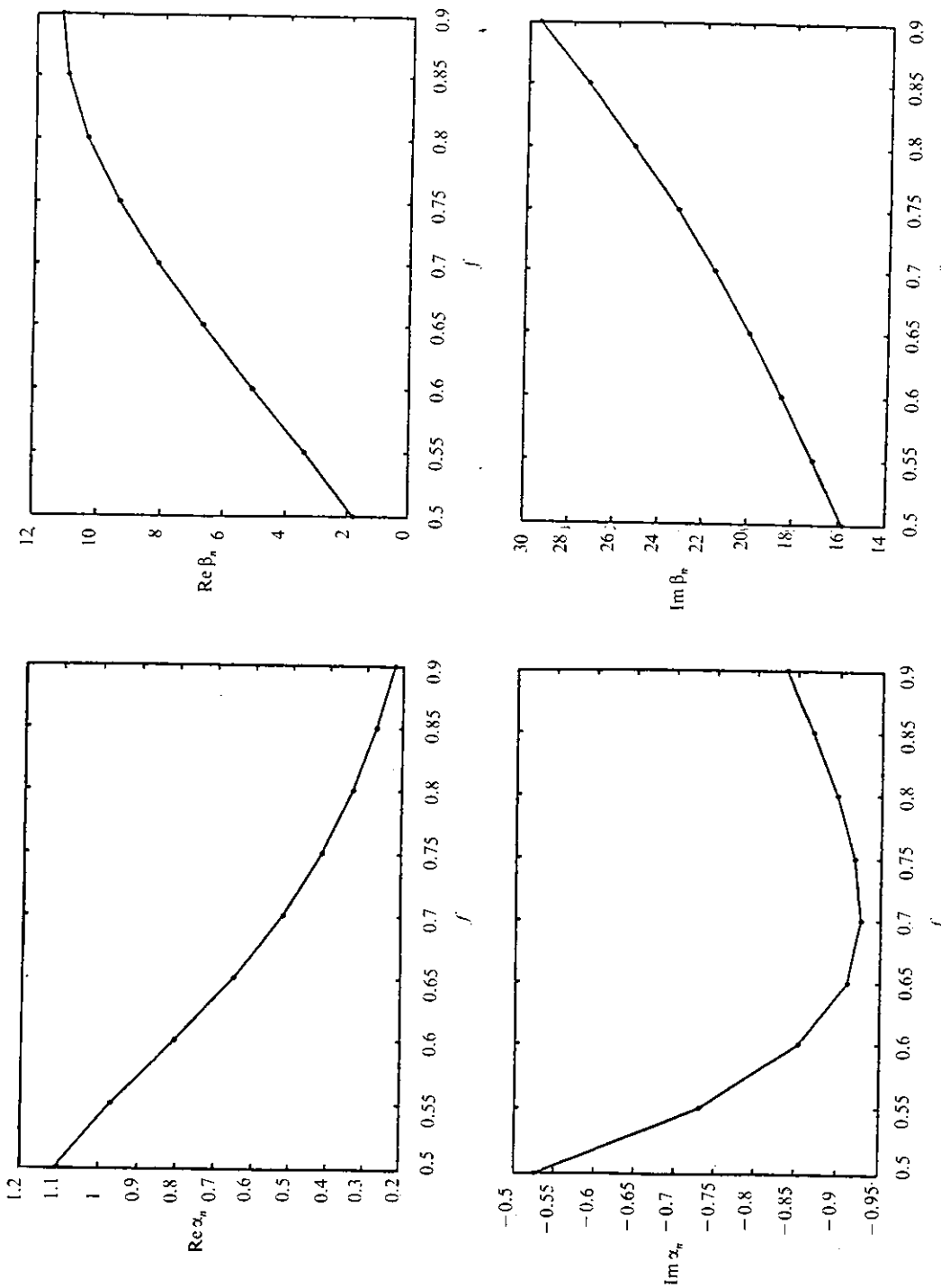

Fig. 6. – Variation of the nonlinear interaction coefficient with the wake deficit parameter for the sinuous mode ($r=0.1$, $p=0$, Re = 700).
Fig. 7. – Variation of the nonlinear interaction coefficient with the wake deficit parameter for the varicose mode ($r=0.1$, $p=0$, Re = 700).

is applicable to the evolution of waves forced at frequencies near the neutral points. When the flow is absolutely unstable the wave numbers with maximum temporal growth rates will dominate. The results in Figures 6 and 7 show that there are no significant qualitative changes in α_n or β_n as f is varied. Calculations were also made for a range of values of p with the fixed values $f=-0.75$, $\mathrm{Re}=700$, and r in order to assess other aspects of wake profile asymmetry. It is seen in Figures 8 and 9 that the coefficients α_n and β_n depart rapidly from their zero values as p departs from zero when there is no imposed shear across the wake (*i.e.*, $r=0$). Nevertheless, the variations with r appear to be more significant than that with p. Most importantly, the sign of terms can be changed for selected combinations of r and p. As noted previously in reference to Figure 5, the coefficient β_n is considerably larger in magnitude than α_n. An important conclusion from these results is that profile asymmetry can have a significant effect on the nonlinear evolution characteristics, particularly for the varicose mode.

There is also some interest to see how the coefficients of the nonlinear terms vary with the Reynolds number. To examine this effect, calculations were made for a fixed wake-shear layer profile ($r=0.1$, $p=0$, $f=-0.75$) over a range of Reynolds numbers. The results in Figure 10 and 11 show that the variations are not monotonic for α_n and that the sign of β_n may change at low Reynolds numbers. Although the change in the imaginary part of α_n is small over the range of Reynolds numbers shown and may not be much greater than the numerical accuracy, the trend is smooth and probably real. We anticipated a consistent asymptotic trend at higher Reynold's numbers which could be extracted from the results, but that is clearly not the case. One may conjecture that α_n is essentially independent of Reynolds number at higher values, but the real and imaginary parts of β_n have different curvatures at the righ Reynolds number end of the graphs. Perhaps the asymptotic regime occurs at higher Reynolds numbers, but the group velocity calculations (*cf.*, Table II) suggest, at least for the Bickley wake profile, that the asymptotic approximation is a good representation at the higher Reynolds numbers in these figures. Of course, the eigenfunctions correspond to regular neutral modes for the Bickley wake ($r=p=0$), but the modes are singular when $r\neq 0$ and/or $p\neq 0$. In the latter case, the asymptotic behaviour may be evident only at much higher Reynolds numbers.

3.3. Group velocity

Calculations of the coefficients D_{ω_α} and D_{k_α}, $\alpha=s, v$, appearing in the evolution model (9 *a*, *b*) were also computed as a function of the different parameters of the problem. We present results here only for the group velocity (14) for selected parameter values. In Figure 12 calculations for wake-shear layers with $p=0$ at fixed Reynolds number are shown. The asymptotic relations (17) for the Bickley wake show that the dependence on the wake deficit parameter f is linear. For the most-part, this linear variation persists for wake shear layers. Only the imaginary part of the group velocity for the sinuous mode departs from the linear behaviour at smaller values of f. Figure 13 shows the behaviour with r and p. In all cases, the dependence of the group velocity on the various parameters is weak relative to the corresponding sensitivity of the nonlinear coefficients α_n and β_n. Another point of interest regarding the group velocity, which is evident in the values given in Table II, is that the calculated values and the asymptotic

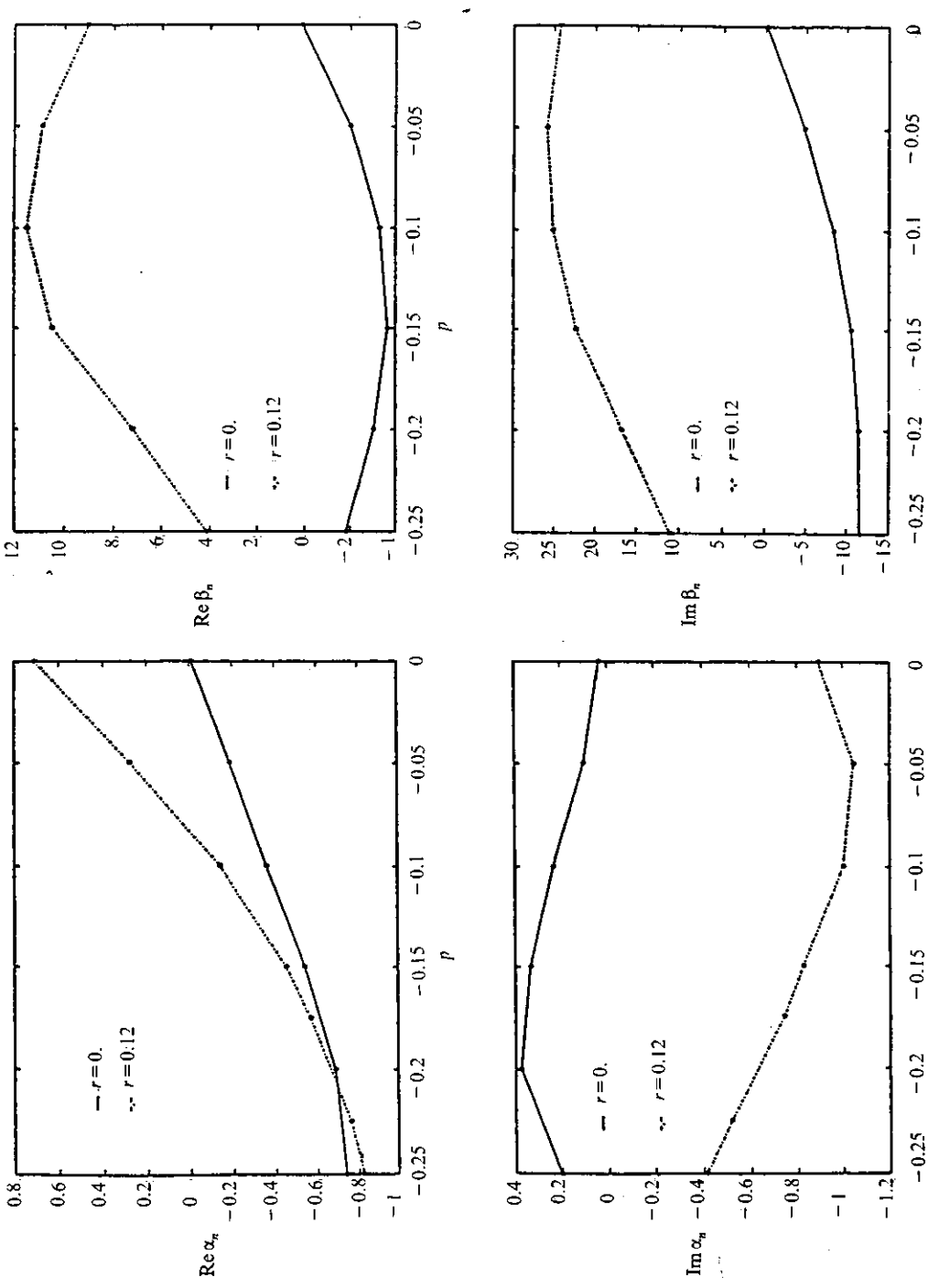

Fig. 8. — Variation of the nonlinear interaction coefficient with asymmetry parameter p for the sinuous mode ($f = -0.75$, Re = 700; — $r = 0$, --●-- $r = 0.12$).

Fig. 9. — Variation of the nonlinear interaction coefficient with asymmetry parameter p for the varicose mode ($f = -0.75$, Re = 700; — $r = 0$, --●-- $r = 0.12$).

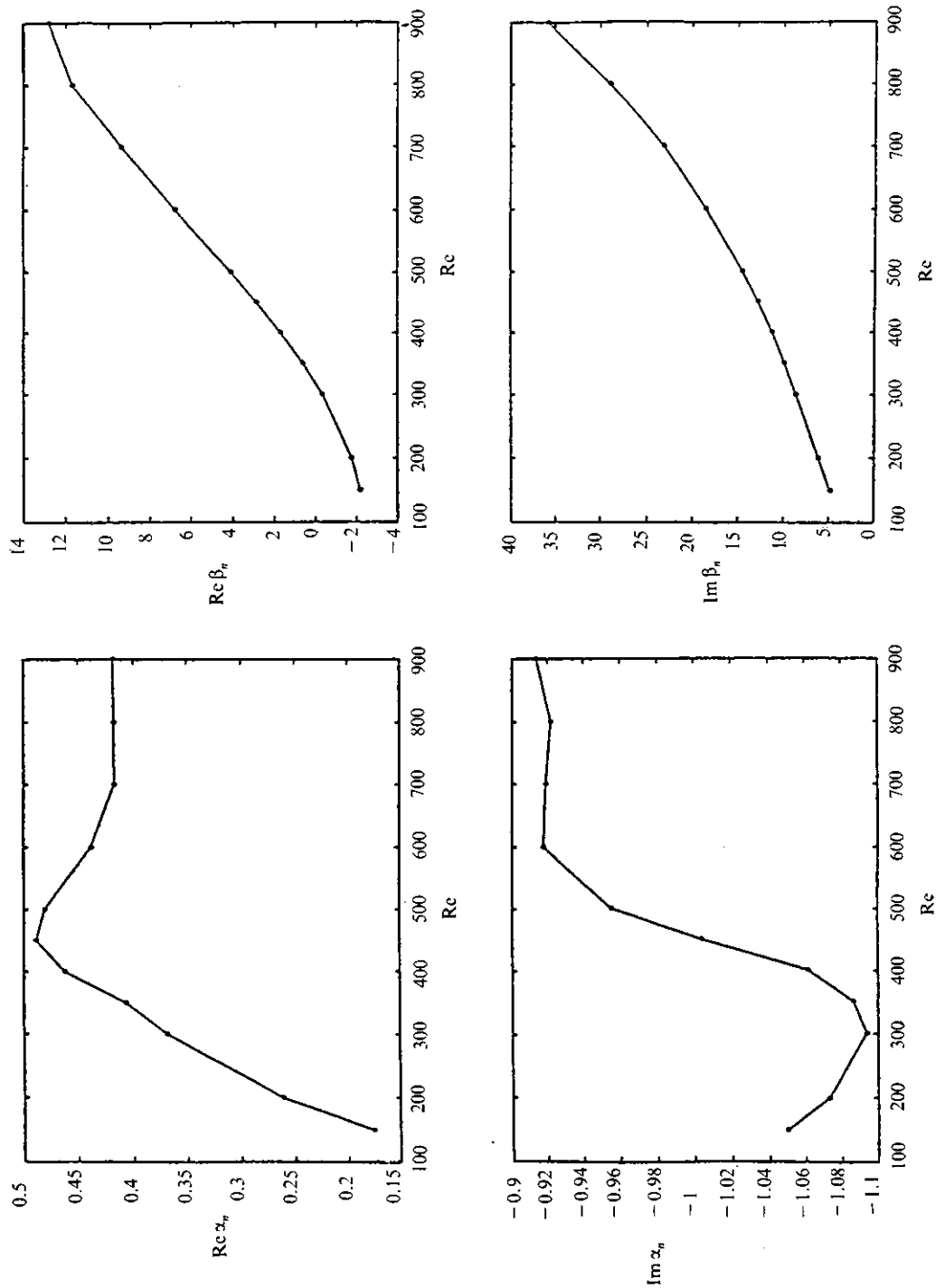

Fig. 10. – Effect of Reynolds number on the nonlinear interaction coefficient for the sinuous mode ($f = -0.75$, $r = 0.1$).

Fig. 11. – Effect of Reynolds number on the nonlinear interaction coefficient for the varicose mode ($f = -0.75$, $r = 0.1$, $p = 0$).

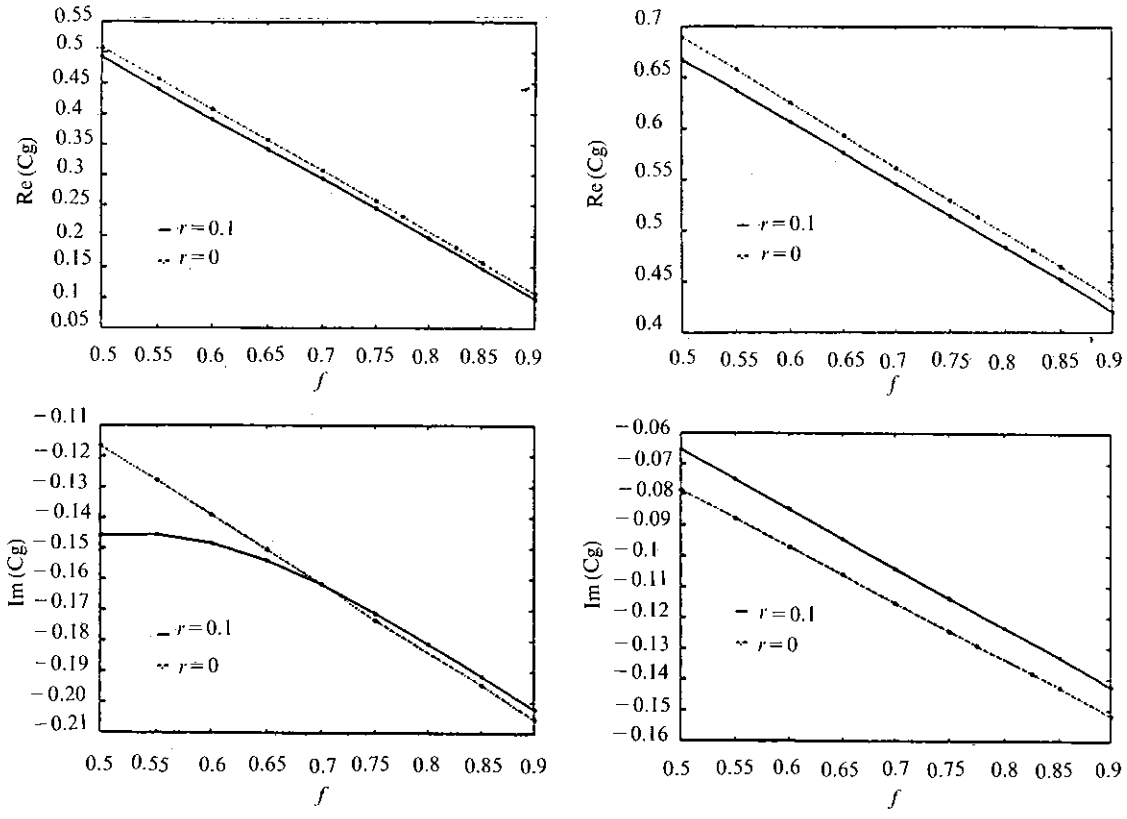

Fig. 12. – Group velocities of the sinuous and varicose modes for wake-shear layers ($p=0$, Re$=700$; $-r=0$, $--\bullet--r=0.1$).

results have the same trend with Reynolds number except for the imaginary part of the sinuous mode. This is exhibited in Figure 14. In each case the computed results converge to the asymptotic values except the imaginary part for the sinuous mode has opposite curvature.

4. Analysis of the evolution system

The evolution system defined by (9 *a*, *b*) is analyzed for a spatially-developing wave system which is temporally periodic. This subclass of solutions is applicable to situations where the sinuous and varicose modes are temporally forced and the system is convectively unstable. The complex amplitudes for the modes are expressed in the form

$$A(X, T) = A_1(X)\, e^{-i(\theta_R + \Omega_s T)} \tag{23 a}$$

$$B(X, T) = B_1(X)\, e^{-i(\theta_R + \Omega_v T)} \tag{23 b}$$

The frequencies Ω_s and Ω_v will be selected to yield specific values for the sinuous and varicose modes, respectively. With these definitions the spatial evolution of the two

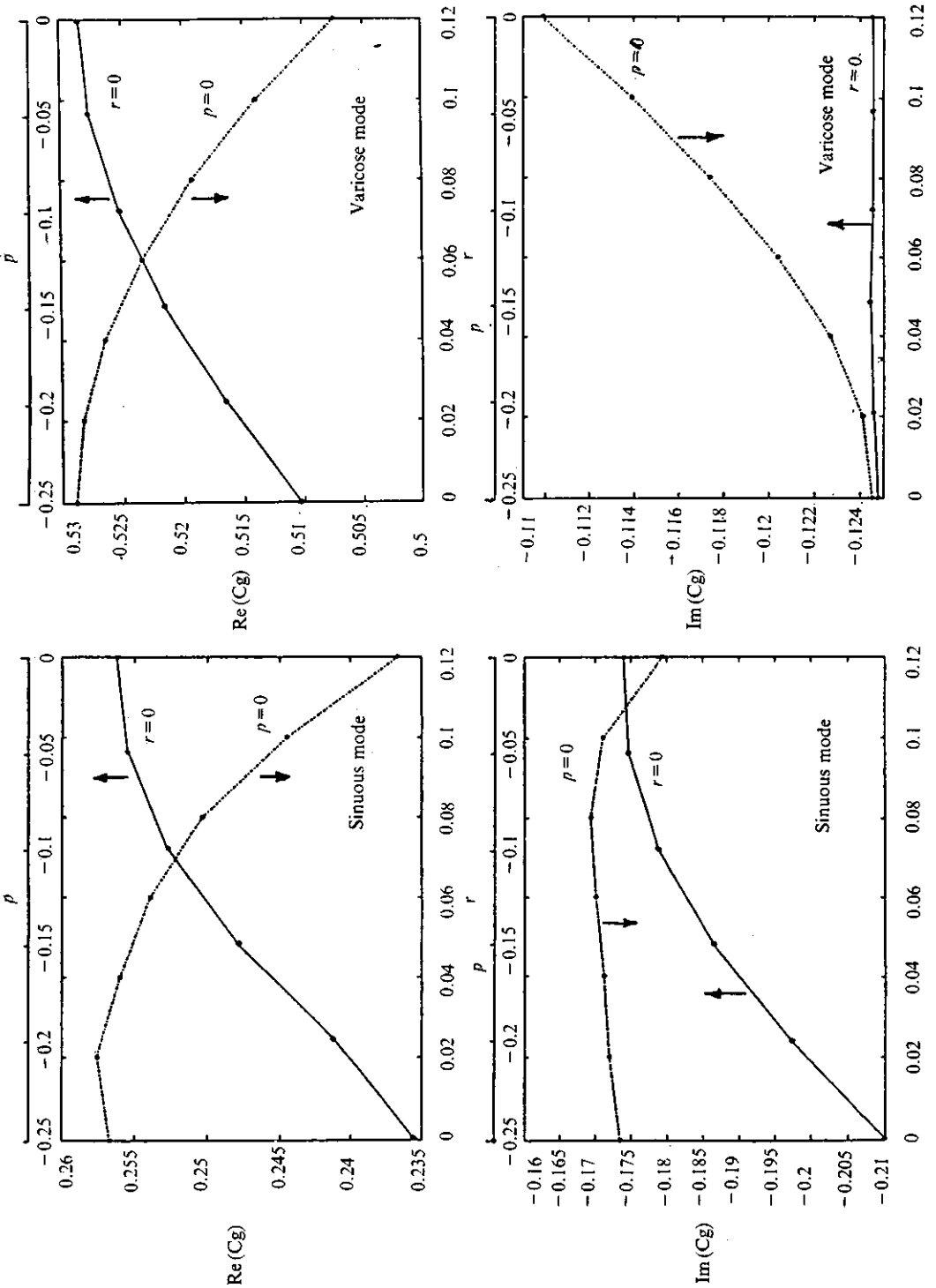

Fig. 13. – Group velocities of the sinuous and varicose modes ($f = -0.75$, Re = 700).

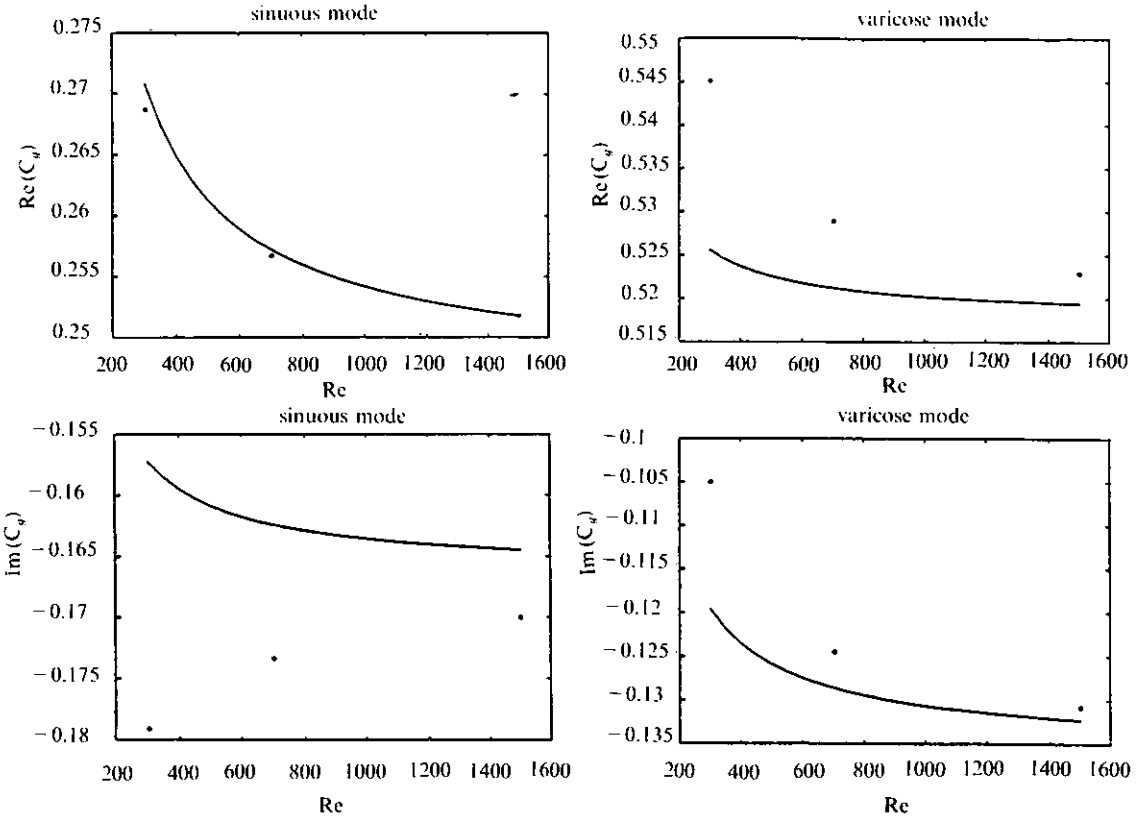

Fig. 14. – Comparison of the computed and asymptotic values of the group velocity ($f=-0.75$, $r=p=0$).

modes is defined by equations which can be cast in the form

$$\frac{dA_1}{dX}=K_s A_1+\rho_s e^{i\phi_s} B_1^2, \tag{24a}$$

$$\frac{dB_1}{dX}=K_v B_1-\rho_v e^{i\phi_v} A_1 \tilde{B}_1 \tag{24b}$$

The variables K_s and K_v are the respective (complex) spatial growth rates and ρ_s, ρ_v, ϕ_s, ϕ_v are the modulus and phase of the coefficients of the nonlinear terms:

$$K_\alpha=K_{\alpha r}+iK_{\alpha i}=\frac{C_{g\alpha i}}{|C_{g_\alpha}|^2}\left[\Omega_\alpha+\frac{\omega_s-2\omega_v}{\varepsilon}\right]+i\left\{\frac{C_{g\alpha r}}{|C_{g_\alpha}|^2}\left[\Omega_\alpha+\frac{\omega_s-2\omega_v}{\varepsilon}\right]-\frac{k_s-2k_v}{\varepsilon}\right\}, \tag{25}$$

$$\alpha=s,\ v,$$

$$\rho_s e^{i\phi_s}=\alpha_n/D_{k_s}, \tag{26a}$$

$$\rho_v e^{i\phi_v}=-\beta_n/Dk_v. \tag{26b}$$

The pair of equations for the complex amplitudes $A_1(X)$ and $B_1(X)$ can be written in terms of three equations for the real variables $a(\xi)$, $b(\xi)$, and $\vartheta(\xi)$, where these functions are defined by the transformations

$$A_1(X) = \frac{K_{sr}}{\rho_v} e^{i\phi_v} a(\xi) e^{i\theta_s(\xi)}, \tag{27a}$$

$$B_1(X) = \frac{K_{sr}}{\sqrt{\rho_s \rho_v}} e^{i\phi_v} b(\xi) e^{i\theta_v(\xi)}, \tag{27b}$$

$$\vartheta(\xi) = \theta_s(\xi) - 2\theta_v(\xi) - \phi_0, \tag{27c}$$

$$\phi_0 = \phi_s + \phi_v, \tag{27d}$$

and

$$\xi = K_{sr} X. \tag{27e}$$

With these definitions the coupled pair of evolution equations can be written in terms of the real, third-order system

$$\frac{da}{d\xi} = a + b^2 \cos\vartheta, \tag{28a}$$

$$\frac{db}{d\xi} = \Gamma b - ab\cos(\vartheta + \phi_0), \tag{28b}$$

$$\frac{d\vartheta}{d\xi} = -\Delta - \frac{b^2}{a}\sin\vartheta + 2a\sin(\vartheta + \phi_0) \tag{28c}$$

where the two new parameters are defined by

$$\Gamma = \frac{K_{vr}}{K_{sr}}, \qquad \Delta = \frac{2K_{vi} - K_{si}}{K_{sr}}. \tag{28d}$$

This dynamical system has the disadvantage that the evolution of the phase $\vartheta(\xi)$ is singular when $a = 0$ (*i.e.*, when the sinuous mode amplitude vanishes). An alternate real form for the system which avoids this difficulty is obtained, following Vyshkind & Rabinovich [1976], through the transformation

$$U(\xi) = a(\xi)\cos(\vartheta(\xi) + \phi_0), \tag{29a}$$

$$V(\xi) = a(\xi)\sin(\vartheta(\xi) + \phi_0), \tag{29b}$$

$$W(\xi) = b^2(\xi). \tag{29c}$$

The system (28 *a*, *b*, *c*) then transforms to

$$\frac{dU}{d\xi} = U + \Delta V - 2V^2 + W\cos\phi_0, \tag{30a}$$

$$\frac{dV}{d\xi} = V - \Delta U + 2UV + W\sin\phi_0, \tag{30b}$$

$$\frac{dW}{d\xi} = -2W(U-\Gamma). \tag{30c}$$

This form proves convenient for numerical calculations.

The interaction of the sinuous and varicose modes in a convectively unstable wake-shear layer has been reduced to a third-order dynamical system for the spatial structure. The system contains three parameters; Δ, Γ, and ϕ_0. Reference to the system (28) shows that the parameter Δ characterizes the wavenumber detuning between the sinuous and varicose modes. With the scaling used here, it is normalized by the spatial growth rate of the sinuous mode. The parameter Γ measures the relative growth rate of the varicose mode and the parameter ϕ_0 measures the phase misfit between the modes. In order to limit the number of independent variables, we assume that the sinuous and varicose modes are forced at frequencies satisfying the condition

$$\omega_{sF} = 2\,\omega_{vF}. \tag{31}$$

This is equivalent to fixing the relation between Ω_s and Ω_v such that

$$\Omega_s = 2\,\Omega_v. \tag{32}$$

With this choice, the parameters in the interaction equations are given by the following relations:

$$\Delta = \frac{C_{g_{sr}}}{C_{g_{si}}}\left\{1 - \frac{|C_{g_{sr}}|^2}{C_{g_{si}}}\cdot\frac{k_s - 2k_v}{\omega_s - 2\omega_v}\right\}\frac{1}{\Omega-1} + \frac{C_{g_{sr}}}{C_{g_{si}}}\left\{\frac{C_{g_{vr}}}{C_{g_{sr}}}\frac{|C_{g_s}|^2}{|C_{g_v}|^2} - 1\right\}\frac{\Omega}{\Omega-1}$$

$$\equiv \frac{g(f, r, p, \mathrm{Re})}{\Omega-1} + \frac{\Omega}{\Omega-1}h(f, r, p, \mathrm{Re}); \tag{33}$$

$$\Gamma = \frac{1}{2}\frac{C_{g_{vi}}}{C_{g_{si}}}\frac{|C_{g_s}|^2}{|C_{g_v}|^2}\frac{\Omega}{\Omega-1} \equiv \frac{\Omega}{\Omega-1}\gamma(f, r, p, \mathrm{Re}); \tag{34}$$

$$\phi_0 = \arg(\alpha_n) + \arg(\beta_n) - \arg(D_{ks}D_{kv}). \tag{35}$$

The control parameter for the system is Ω which is a dimensionless forcing frequency defined as

$$\Omega = \frac{\omega_{vF} - \omega_v}{\frac{1}{2}\omega_s - \omega_v} = \frac{\mu - 1}{s - 1}, \tag{36}$$

where $\mu = \dfrac{\omega_{vF}}{\omega_v}$ and $s = \dfrac{\omega_s}{(2\,\omega_v)}$. It is readily apparent that this parameterization is not useful when the neutral frequencies satisfy the precise resonance condition $\omega_s = 2\,\omega_v$. The quantities Δ and Γ are, however, still well-behaved in this limit. An alternate parameterization which avoids the difficulties associated with this resonance condition when $s = 1$ makes use of μ as the control parameter.

Then,

$$\Delta = \frac{1}{\mu - s}\frac{C_{g_{sr}}}{C_{g_{si}}}\left\{\frac{C_{g_{vr}}}{C_{g_{sr}}}\frac{|C_{g_s}|^2}{|C_{g_v}|^2}(\mu - 1) - (\mu - s) - \frac{|C_{g_s}|^2}{C_{g_{sr}}C_v}(d-1)\right\} \tag{37}$$

and

$$\Gamma = \frac{1}{2}\frac{\mu - 1}{\mu - s}\frac{C_{g_{vi}}}{C_{g_{si}}}\frac{|C_{g_s}|^2}{|C_{g_v}|^2} \tag{38}$$

The parameter d appearing in (37) is defined by $d = \dfrac{k_s}{(2k_v)}$, the resonant wave-number ratio. The singular behaviour of these coefficients when $\mu = s$ arises because of the scaling associated with the independent variable ξ (*cf.*, eq'*n*.27*e*) which can be expressed as

$$\xi = K_{sr}X = \frac{C_{g_{si}}}{|C_{g_s}|^2}\frac{\omega_{sF} - \omega_s}{\varepsilon}X = \frac{2C_{g_{si}}}{|C_{g_s}|^2}\omega_v(\mu - s)x. \tag{39}$$

The divergence of the flow defined by the dynamical system (30) is equal to $2(1+\Gamma)$ implying that trajectories are unbounded for $\Gamma > -1$. For $\Gamma < -1$ volume elements in phase space contract and bounded solutions are possible. There are two classes of fixed points for the system; the origin and those sets associated with $U = \Gamma$ in (30*c*). The origin is always unstable while the fixed points associated with $U = \Gamma$ are stable for a restricted range of the parameters (Δ, Γ, ϕ_0). Outside this range of parameters the system exhibits either attracting solutions which undergo an infinite sequence of period-doubling bifurcations leading to chaotic dynamics or else solutions which are unbounded. In that domain of parameter space where solution trajectories are unbounded, the model (30) loses physical relevance and must be augmented with higher-order terms (*i.e.*, cubic nonlinearities). The present system has been examined in some detail by Wersinger, Finn & Ott [1980]. The dynamical model (28) or (30) has also been studied independently by Saulière & Huerre [1987] and more recently by Proctor & Hughes [1990] and Hughes & Proctor [1993]. In the domain of attracting solutions, these investigators were able to reduce the dynamical system to a one-dimensional map through asymptotic analyses. These are remarkable achievements in that they provide specific examples where the Navier-Stokes system is asymptotically equivalent to a one-dimensional map containing bifurcation sequences leading to complex dynamics. Further detailed studies of the dynamics represented by (30) will not be attempted here except for the one sample result shown in Figure 15. This figure shows a portion of the space of attracting solutions which are possible for a fixed choice of ϕ_0. The dynamics implicit in this part of parameter space involve periodic or intermittent bursts of the varicose mode. In this case the dynamical system describes a periodically-forced, spatially-developing array of vortex structures where the regularity of the vortex street associated with the sinuous mode is interrupted at spatial positions with significant content of the varicose mode. In the chaotic region, a spatially-chaotic arrangement of vortices exists.

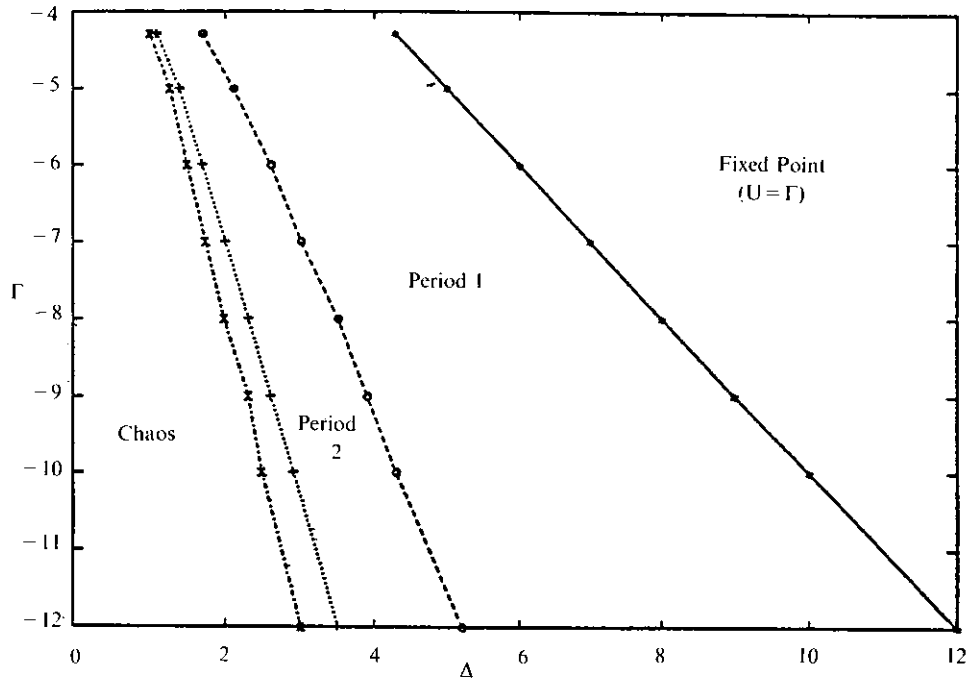

Fig. 15. – A representative space pf attracting solutions ($\phi_0 = \pi/10$).

5. The evolution model for wake-shear layers

The evolution model described in the preceding section has been employed to examine the (near) resonant coupling of the sinuous and varicose modes in a forced, spatially-developing, wake-shear layer. In particular, the dynamical system (30) was studied with Ω as the control parameter for a wake-shear layer with $r=0.1$, $p=0$, and $\mathrm{Re}=700$. Since the wake deficit decreases with increasing distance in any spatially-developing wake-shear layer, the coefficients in the dynamical system were evaluated for a range of values for f.

Referring to equations (33)-(35), four functions (g, h, γ and ϕ_0), each of which depend on the parameters defining the character of local mean velocity profiles, are required to specify the dynamical system for a fixed value of the control parameter. Calculations of these functions based on results presented in Section 3 are shown in Figure 16. The singular behaviour of the function g for the chosen value of the velocity ratio and the Reynolds number when the wake-deficit parameter is around $f=-0.7$ shows that the neutral frequencies satisfy the resonance condition $\omega_s = 2\omega_v$ for these conditions. The remaining functions h, γ and ϕ_0 are well-behaved. The significant result from these calculations vis-à-vis the dynamical system (30) is the relative values of Δ and Γ. Elimination of the control parameter Ω in (33) and (34) leads to the relation $\Delta = \dfrac{g+h}{\gamma}\Gamma - g$. The small value of γ in the present case places the parameters Δ and Γ in a domain where the dynamical system has unbounded trajectories, at least for the

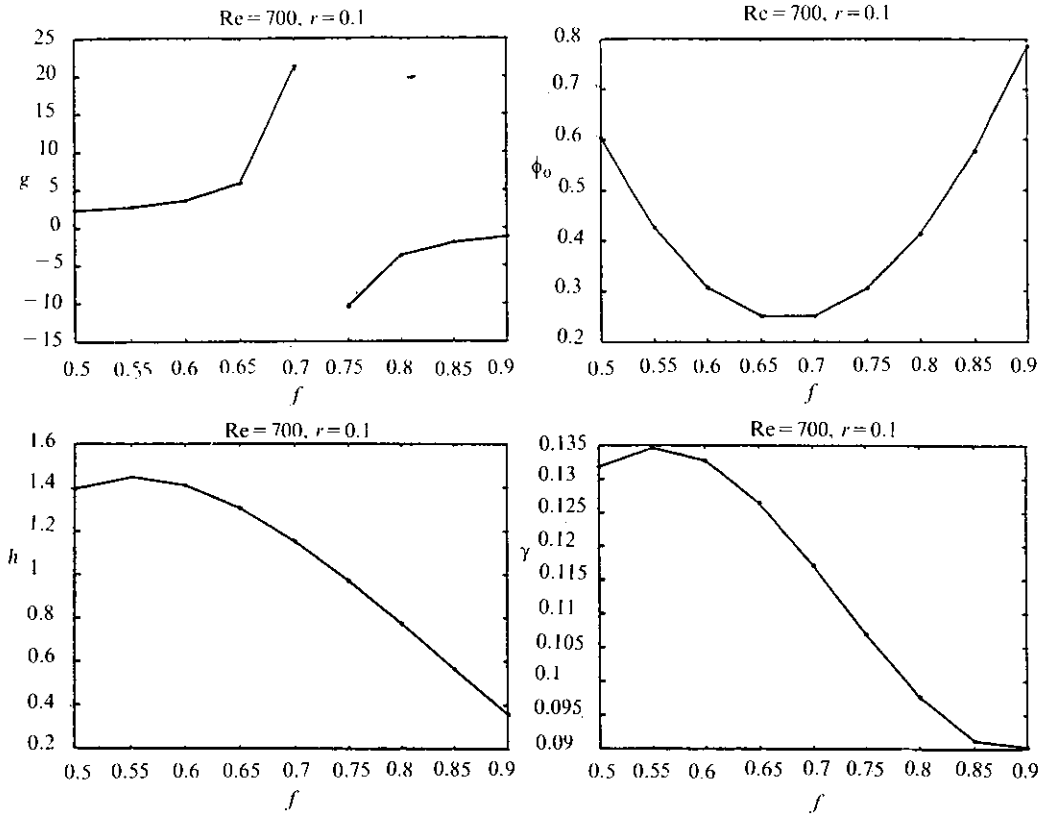

Fig. 16. – Velocity profile parameters functions ($r = 0.1$, $p = 0$, Re = 700).

chosen values of r, p and Re. In this instance, an extended evolution system along the lines derived by Proctor & Jones [1988] in their study of spatially-resonant states in thermal convection is necessary. Evaluation of these parameters for other choices of f, r, p and Re could be accomplished to ascertain a possible family of profiles for which the evolution model (30) has asymptotic validity. However, it is felt that such an exercise is not warranted at this stage. A more meaningful effort would involve computation of higher-order terms in amplitude equations. To extend the present model along those lines requires restrictive assumptions concerning the parallel nature of the mean flow. In this connection, a preferred approach to the interaction of the sinuous and varicose modes in a spatially-developing flow would, perhaps, be that adopted by Leib & Goldstein [1989].

6. Concluding remarks

The resonant interaction between the sinuous and varicose modes in wake-shear layers has been studied for finite Reynolds numbers. It is shown that the broken symmetry of the velocity profile at small velocity ratios can lead to a strong nonlinear coupling of the

modes. The broken symmetry forces the neutral modes to be singular on an inviscid basis with consequent strong nonlinear interaction in the critical layer region at finite Reynolds numbers. The present results suggest that even weak asymmetries can stimulate significantly altered nonlinear development of flow instabilities or forced response. These conclusions await further experimental and/or numerical investigations.

Several experimental studies have pointed to the significance of the nonlinear coupling between the sinuous and varicose modes in a wake. Ongoren & Rockwell [1988] studied the laminar wake behind a cylinder at an oblique angle α to the flow and forced at frequency ω_F. For particular values of α and the frequency ratio ω_F/ω_N, where ω_N is the natural frequency, the near-wake structure was completely synchronized in either of the modes. For values of the frequency ratio below one-half, however, the varicose mode appeared only very intermittently in short-duration pulses. As the frequency ratio was gradually increased, the duration of the bursts of varicose-mode activity lengthened until both modes became equally probable. Wygnanski, Champagne & Marasli [1986] have argued strongly that both the sinuous and varicose modes should be included in a description of the vortical structures in small-deficit turbulent wakes. They note that a simple linear "superposition of the two modes of instability leads to physically acceptable flow patterns associated generally with large coherent structures contained in the wake" for deficit parameters in the range $-0.15<f<-0.03$. It was hypothesized by these authors that the lack of universality of the far wake results from the interaction between these modes. The present work suggests that weak asymmetries could be a contributing factor, as well as possible spatial intermittency of the varicose mode, through nonlinear coupling.

Acknowledgements

The authors gratefully acknowledge support obtained from the U.S. Air Force Office of Scientific Research under Grant No. F49620-85-C-0080. D. W. also acknowledges the support of a Rockwell International Graduate Fellowship. Discussions with Dr. M. Rossi and J. Saulière were very helpful in the earlier stages of this work.

REFERENCES

AREF H., GHARIB M., VAN ATTA C. W., 1987, Chaos in shear flows, AIAA Paper 87-1251.

CHURILOV S. M., SHUKHMAN I. G., 1987. Note on weakly nonlinear stability theory of a free mixing layer. *Proc. Roy. Soc. London*, **A409,** 351-367.

DJORDJEVIC V. D., Redekopp L. G., 1990, Effect of profile symmetry on the nonlinear stability of mixing layers, *Stud. Appl. Math.*, **83**, 287-317.

DJORDJEVIC V. D., REDEKOPP L. G., 1994, *The nonlinear development of a singular neutral mode in a subsonic shear flow* (to appear).

DRAZIN P. G., REID W. H., 1981, *Hydrodynamic stability*, Cambridge Univ. Press.

HUGHES D. W., PROCTOR M. R. E., 1993, Nonlinear three-wave interaction with non-conservative coupling, *J. Fluid Mech.*, **244,** 583-604.

HUERRE P., 1980, The nonlinear stability of a free shear layer in the viscous critical layer regime, *Phil. Trans. Royal Society London*, **A293,** 643-675.

HUERRE P., 1987, On the Landau constant in mixing layers, *Proc. Roy. Soc. London*, **A409,** 369-381.

KELLY R. E., 1968, On the resonant interaction of neutral disturbances in two inviscid shear flows, *J. Fluid Mech.*, **31,** 789-799.

LEIB S. J., GOLDSTEIN M. J., 1989, Nonlinear interaction between the sinuous and varicose instability modes in a plane wake, *Phys. Fluids A*, **1,** 513-521.

MONKEWITZ P. A., 1988, The absolute and convective nature of instability in two-dimensional wakes at low Reynolds numbers, *Phys. Fluids*, **31,** 999-1006.

OLLINGER D. J., SREENIVASAN K. R., 1988, Nonlinear dynamics of the wake of an oscillating cylinder, *Phys. Rev. Lett.*, **60,** 797-800.

ONROGEN A., ROCKWELL D., 1988, Flow structure from an oscillating cylinder. Part 2. Mode competition in the near wake, *J. Fluid Mech.*, **191,** 225-245.

PROCTOR M. R. E., HUGHES D. W., 1993, Chaos and the effect of noise for the double Hopf bifurcation with 2:1 resonance. In *Nonlinear evolution of spatio-temporal structures in dissipative continuous systems* (H. Busse and L. Kramer Ed.), Plenum, 375-384.

PROCTOR M. R. E., Jones C. A., 1988, The interaction of two spatially resonant patterns, Part. 1. Exact 1:2 resonance, *J. Fluid Mech.*, **188,** 301-335.

SAULIÈRE J., HUERRE P., 1987, Spatial chaos and nonlinear interactions in wake-shear layers, *Bull. Am. Phys. Soc.*, **32,** 2071.

VAN ATTA C. W., GHARIB M., HAMMACHE M., 1988, Three-dimensional structures of ordered and chaotic vortex streets behind circular cylinders at low Reynolds numbers, *Fluid Dyn. Res.*, **3,** 127-132,

VYSHKIND S. R., RABINOVICH M. J., 1976, The phase stochastization mechanism and the structure of wave turbulence in dissipative media, *Sov. Phys., J. Exp. Theor. Phys.*, **44,** 292-299.

WALLACE D., REDEKOPP L. G., 1991, Linear instability characteristics of wake-shear layers, *Phys. Fluids A*, **4,** 189-191.

WERSINGER J. M., FINN J. M., OTT E., 1980, Bifurcation and "strange" behavior in instability saturation by nonlinear three-wave mode coupling *Phys. Fluids*, **23,** 1142-1154.

WILLIAMS-STUBER K., GHARIB M., 1989, Experiments on the forced wake of an airfoil, *J. Fluid Mechanics*, **208,** 225-255.

WYGNANSKI I., CHAMPAGNE F., MARASLI B., 1986, On the large-scale structures in two-dimensional, small-deficit, turbulent wakes, *J. Fluid Mech.*, **168,** 31-71.

ZHANG Y.-Q., HO C.-M., MONKEWITZ P. A., 1985, The mixing layer forced by fundamental and subharmonic, *Laminar-Turbulent Transition* (V. V. Kozlov Ed.), 385-395, Springer, Berlin.

(Manuscript received March 25, 1993;
accepted April 20, 1993.)